J. Am. Soc. Mass Spectrom. (2017) 28:2124–2131
DOI: 10.1007/s13361-017-1737-5

RESEARCH ARTICLE

The Evolution of Electrospray Generated Droplets is Not Affected by Ionization Mode

Piia Liigand,[1] Agnes Heering (Suu),[1] Karl Kaupmees,[1] Ivo Leito,[1] Marion Girod,[2] Rodolphe Antoine,[3] Anneli Kruve[1,4]

[1]Institute of Chemistry, University of Tartu, Ravila 14a, 50411, Tartu, Estonia
[2]CNRS, Université Claude Bernard Lyon 1, Ens de Lyon, Institut des Sciences Analytiques, University of Lyon, UMR 5280, 5 rue de la Doua, F-69100, Villeurbanne, France
[3]Université Claude Bernard Lyon 1, CNRS, Institut Lumière Matière, University of Lyon, UMR 5306, F-69622, Lyon, France
[4]Schulich Faculty of Chemistry, Technion-Israel Institute of Technology, Technion City, Haifa, 3200008, Israel

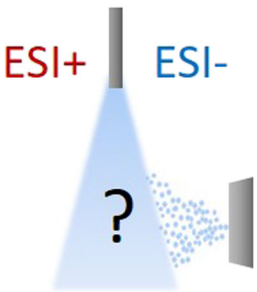

Abstract. Ionization efficiency and mechanism in ESI is strongly affected by the properties of mobile phase. The use of mobile-phase properties to accurately describe droplets in ESI source is convenient but may be inadequate as the composition of the droplets is changing in the plume due to electrochemical reactions occurring in the needle tip as well as continuous drying and fission of droplets. Presently, there is paucity of research on the effect of the polarity of the ESI mode on mobile phase composition in the droplets. In this paper, the change in the organic solvent content, pH, and droplet size are studied in the ESI plume in both ESI+ and ESI– ionization mode. We introduce a rigorous way – the absolute pH ($pH_{abs}^{H_2O}$) – to describe pH change in the plume that takes into account organic solvent content in the mobile phase. $pH_{abs}^{H_2O}$ enables comparing acidities of ESI droplets with different organic solvent contents. The results are surprisingly similar for both ionization modes, indicating that the dynamics of the change of mobile-phase properties is independent from the ESI mode used. This allows us to conclude that the evolution of ESI droplets first of all proceeds via the evaporation of the organic modifier and to a lesser extent via fission of smaller droplets from parent droplets. Secondly, our study shows that qualitative findings related to the ESI process obtained on the ESI+ mode can almost directly be applied also in the ESI– mode.

Keywords: Mass spectrometry, Fluorescence spectroscopy, Plume profiling

Received: 6 April 2017/Revised: 22 May 2017/Accepted: 11 June 2017/Published Online: 25 July 2017

Introduction

It has been observed that different solvents have different influence on ionization in electrospray ionization mass spectrometry (ESI/MS) analysis [1, 2]. Most often acetonitrile or methanol in a mixture with water are used as mobile phase in ESI. It has been shown that in many cases ESI response is higher in solutions with higher organic modifier percentage [3]. This may be due to more efficient desolvation of the droplets, allowing them to reach Rayleigh limit faster and eventually generate smaller droplets more rapidly [4].

pH of the mobile phase also influences ionization in the ESI plume [5]. It has been established that in general, basic analytes provide higher sensitivity with more acidic mobile phase in ESI positive mode (ESI+) and acidic analytes with more basic mobile phase in ESI negative mode (ESI–) [2]. It has also been shown that protonated forms of basic analytes can frequently be observed even if the pK_a (of the protonated analyte) is far below the solution's pH [6–8]. Similarly, deprotonated forms of analytes can be observed when ESI/MS analysis is performed with acidic solutions with pH lower than the analyte pK_a [6, 9]. Therefore, pH is an important parameter influencing ionization.

In terms of the mobile phase, the initial composition is generally used to describe the ESI process as the actual composition in the plume is difficult to measure. However, it has been shown that solvent pH [10–13], organic modifier content [8, 14–17], and droplet size [14, 17–19] change along the plume. The complex dynamics of the ESI process make the transition of ions from solution-phase to gas-phase difficult to model. Atomistic molecular dynamics methods for such simulations have been used [20–25], but are usually limited to the droplets containing up to a few thousand solvent molecules.

Correspondence to: Piia Liigand; *e-mail:* piia.liigand@ut.ee

Therefore, it is advantageous to directly perform optical spectroscopic measurements of physicochemical parameters of droplets and their changes in the electrospray plume in order to correlate the ions observed in the initial sample solution to those observed in the gas phase by the mass spectrometer.

Fluorescence excitation studies of octaethylporphyrin in the electrospray stream pioneered in using spectroscopy to describe the processes in ESI plume [26]. More recently, several researchers [10, 11, 15–18, 27] have developed laser-induced fluorescence strategies to probe properties of ESI plume, e.g., solvent fractionation, solvent polarity, pH, and temperature, and correlate changes with droplet size evolution along the ESI plume. Whereas these experiments were performed by mimicking electrospray sources (i.e., without actual MS measurements), there have also been studies on the aforementioned changes in combination with mass spectrometry [8, 12–14, 19].

Previous studies have measured either aqueous phase pH or the pH of the mobile phase (mixture of water phase and organic solvent) using calibration in water phase. Depending on the organic modifier, it can significantly influence the pH of the solvent mixture, indicating that the conclusions drawn from the aqueous phase pH might be oversimplified. We improve upon the conventional approach by for the first time profiling the pH in the spray according to the absolute pH scale [28]. It is expressed as $pH_{abs}^{H_2O}$ values [29], which enables direct comparison of the pH between different solvents and water (see Experimental section). The acidity of solvent composition was probed in the aqueous pH ($^{w}_{w}$pH, refers to the "conventional" pH calibrated and measured in water) range from 3.21 to 5.16 using pH-chromic fluorescent dye as the molecular probe.

ESI+ and ESI– modes have only rarely been profiled simultaneously [10–12, 18], but the ESI spray parameters used between modes are different, also only ref [12] uses ESI coupled with mass spectrometer. Zhou et al. [10, 11] and Girod et al. [12] studied the pH change in water droplets, and Wortmann et al. [18] compared the droplet size for acetonitrile droplets for ESI+ and ESI–. However, usually mobile phase contains both water and organic solvent and the evolution of several parameters – pH, organic modifier content, droplet size – occurs simultaneously. Despite the fact that most ESI studies are carried out with acidic mobile phase, these studies have the lowest initial pH of 6.5 [12].

The aim of this study is to quantify the changes occurring in the ESI plume: organic modifier percentage, pH, as well as droplet size change of the "parent" ESI droplets with the diameter range of a few micrometers. For quantitative comparison of pH changes, the absolute pH is used, which enables comparing different solvents and solvent compositions. Even more so, we will estimate whether ESI polarity affects the magnitude of mobile-phase properties' change in the ESI plume. This enables for the first time comparing the processes occurring in ESI source and aids in better understanding of the differences and similarities of the two modes. This work is novel in three aspects: (1) the most acidic mobile phases are studied, (2) we use an identical set of ESI source parameters for both ESI+ and ESI–, thereby enabling accurate and direct comparison between the two modes, (3) we use absolute pH, enabling to accurately compare mobile phases with different organic-phase content and different aqueous pH.

Experimental

Absolute pH Theory

The conventional pH is defined by IUPAC [30] as given in Equation 1:

$$\mathrm{pH} = -\log a_H \tag{1}$$

where a_H is the relative activity in molar scale. This means that the zero point (standard state) of pH scale is activity of 1 mol/kg of H^+_{solv} *in the given solvent* (or solvent mixture). Therefore, every solvent or solvent mixture has its own pH scale and none of these scales are comparable because of unknown shifts of the zero points. To add confusion to these different pH scales, there is the question of calibration, which leads to another possibility to define or name pH scales as $^{s}_{s}$pH or $^{s}_{w}$pH, where subscript shows calibration and superscript measurement medium (s is solvent and w is water). This question is discussed in detail by Rosés [31].

Recently, Himmel et al. proposed a unified acidity scale that is based on the absolute standard chemical potential $\mu_{abs}(H^+)$ of the solvated proton [28] and where the zero point of the scale is the $\mu_{abs}(H^+)$ of the proton in the gas phase, which is arbitrarily set to 0 kJ mol^{-1}. Importantly, this zero point of the scale is universal to all possible media, thereby enabling comparison of the acidities of any given media on one scale. In any solvent, the chemical potential of the proton is decreased (becomes more negative) by solvation. The more negative the proton's chemical potential, the lower is its activity and consequently the acidity of the solution. The absolute acidity (absolute pH, pH_{abs}) can be calculated via the solvated proton's chemical potentials as follows:

$$\mathrm{pH_{abs}} = -\frac{\mu_{abs}(\mathrm{H^+,\ solv})}{RT\ \ln 10} \tag{2}$$

where R is the molar gas constant, T is the absolute temperature, and $\mu_{abs}(H^+,solv)$ is calculated as given in Equation 3,

$$\mu_{abs}(\mathrm{H^+,\ solv}) = \Delta_{solv}G^{\ominus}(\mathrm{H^+}) - [\mathrm{pH} \times RT\ln 10] \tag{3}$$

where $\Delta_{solv}G^{\ominus}(H^+)$ is Gibbs energy of solvation and pH is the conventional pH. This approach is also fully universal in the sense that it does not set any limitations to the solvation sphere of the proton. At the same time, the properties of the solvation sphere (extent of solvation) of the proton are explicitly taken into account by the decrease of chemical potential.

As was said by IUPAC already in 1985 [32] an "intersolvental" pH scale would be ultimately referenced to water due to the indisputable key role of water as a solvent. For

the same reason, absolute acidity is linked to water pH scale via Gibbs energy of solvation as follows:

$$pH_{abs}^{H_2O} = pH_{abs} + \frac{\Delta_{solv}G^{\ominus}(H^+, H_2O)}{RT\ln 10} \quad (4)$$

The notion $pH_{abs}^{H_2O}$ means that pH is expressed on the absolute scale, but values are shifted by a constant in order to make the pH_{abs} values directly comparable to the conventional aqueous pH values (i.e., $pH_{abs}^{H_2O}$ value 7.00 refers to the acidity of the solution where the proton's chemical potential is as high as in aqueous solution with ${}^{w}_{w}$pH 7.00). Thus the unified pH scale enables expressing acidity of any media on a unified scale in the form of familiar aqueous pH (${}^{w}_{w}$pH) values.

Absolute pH Measurements

Absolute pH values (Table 1) were obtained by using a Metrohm 713 pH meter in differential potentiometry mode with two metal-coated glass electrodes (Laboratory of Glass Electrochemistry, St. Petersburg State University) as described in [29]. Measurements were made at (25 ± 1) °C. Consistency standard deviation of the results was 0.01 pH units and in total 52 measurements were made. Liquid junction potentials and uncertainties were calculated as in ref [29]. Absolute pH values were measured in bulk solutions and used as reference for calibrating $pH_{abs}^{H_2O}$ in the plume.

Table 1. The acidity of mobile phases expressed as $pH_{abs}^{H_2O}$ values together with measurement uncertainties

Mobile phase[a]	$pH_{abs}^{H_2O}$	u_{RW} [b]	u_C [c]
MeCN/ ${}^{w}_{w}$pH 5.50 80/20	8.59	0.01	0.14
MeCN ${}^{w}_{w}$pH 5.00 80/20	8.43	0.01	0.14
MeCN/ ${}^{w}_{w}$pH 5.50 75/25	8.41	0.01	0.14
MeCN/ ${}^{w}_{w}$pH 5.50 70/30	8.23	0.01	0.14
MeCN/ ${}^{w}_{w}$pH 5.00 75/25	8.18	0.01	0.14
MeCN/ ${}^{w}_{w}$pH 4.50 80/20	8.10	0.01	0.14
MeCN/ ${}^{w}_{w}$pH 5.00 70/30	7.94	0.01	0.14
MeCN/ ${}^{w}_{w}$pH 4.50 75/25	7.80	0.01	0.14
MeCN/ ${}^{w}_{w}$pH 4.00 80/20	7.64	0.01	0.14
MeCN/ ${}^{w}_{w}$pH 4.50 70/30	7.50	0.01	0.14
MeCN/ ${}^{w}_{w}$pH 5.50 50/50	7.49	0.01	0.14
MeCN/ ${}^{w}_{w}$pH 4.00 75/25	7.32	0.01	0.14
MeCN ${}^{w}_{w}$pH 5.50 45/55	7.30	0.01	0.14
MeCN/ ${}^{w}_{w}$pH 3.50 80/20	7.18	0.01	0.14
${}^{w}_{w}$pH 7 (diluted)	7.13	0.01	0.14
MeCN/ ${}^{w}_{w}$pH 5.50 40/60	7.11	0.01	0.14
MeCN/ ${}^{w}_{w}$pH 5.00 50/50	7.05	0.01	0.14
MeCN/ ${}^{w}_{w}$pH 4.00 70/30	7.03	0.01	0.14
MeCN/ ${}^{w}_{w}$pH 3.50 75/25	6.86	0.01	0.14
MeCN/ ${}^{w}_{w}$pH 5.00 45/55	6.85	0.01	0.14
MeCN/ ${}^{w}_{w}$pH 5.00 40/60	6.62	0.01	0.14
MeCN/ ${}^{w}_{w}$pH 3.50 70/30	6.57	0.01	0.14
MeCN/ ${}^{w}_{w}$pH 4.50 50/50	6.56	0.01	0.14
MeCN/ ${}^{w}_{w}$pH 4.50 45/55	6.36	0.01	0.14
MeCN/ ${}^{w}_{w}$pH 4.50 40/60	6.14	0.01	0.14

[a] The aqueous phase is 0.1% formic acid solution titrated with 25% ammonia solution to the desired ${}^{w}_{w}$pH

[b] Within-lab reproducibility estimates (u_{RW}) can be used to evaluate the internal consistency of the measured values

[c] These combined standard uncertainty estimates (u_C) can be used to compare the acidities of the solutions in this scale with the acidities of aqueous solutions by conventional pH measurement

ESI Plume Profiling

Acetonitrile (MeCN) content was profiled in ESI+ and ESI– for solutions initially containing 80% and 50% MeCN (v/v) from fluorescent measurements of the solvatochromic dye Nile Red [14]. pH was profiled for mobile phases with initial compositions of acetonitrile/aqueous solution with ${}^{w}_{w}$pH of 5.03 in the ratio of 80/20 and 50/50, and also for 80/20 mixture with aqueous solution with ${}^{w}_{w}$pH of 4.00. The corresponding $pH_{abs}^{H_2O}$ changes are listed in Table 2. The change of the droplet size was studied for the same mobile phases.

The experimental setup profiling the spray plume consists of an excitation laser and two different optical detection systems mounted on a moving stage. It is coupled with a Single Quad 6100 mass spectrometer equipped with a modified Agilent Jet Stream ESI source (Agilent Technologies, Santa Clara, CA, USA) in order to allow the laser injection into the plume and the epifluorescence measurements. Used ESI parameters were: capillary voltage 3500/–3500 V, nebulizing gas pressure 15 psi, drying gas flow rate 7 L/min, drying gas temperature 300 °C, sheath gas flow rate 1 L/min, and temperature 80 °C. Solutions were introduced in the ionization source at 50 μL min^{-1} flow rate with a KDS100 syringe pump (KD Scientific, Holliston, MA, USA).

A continuous laser (λ = 473 nm) emitting in a single longitudinal mode was used to profile ESI plume. The output power of the laser is around 500 mW and its beam diameter is 1.5 mm (divergence 1 mrad). The laser is injected through the objective using two reflecting protected aluminum flat mirrors (R > 90%). The laser beam is focused into the spray and the fluorescence is collected via an objective used in an epifluorescence configuration. Fluorescence spectra from ESI plume were recorded, point by point (pixel size 500 μm), by an ultra-compact spectrophotometer (B&WTek Inc., Newark, DE, USA). The plume was profiled for 15 mm starting from ESI needle tip, except for 50% MeCN solution, where plume was profiled for 13 mm because of poor solubility of the fluorescent probe.

The obtained raw data was processed using OriginPro 7.0 software. Profiles of pH and solvent composition in the ESI plume (Figure 1a and b) were determined from calibrations in different solutions.

For droplet size profiling (Figure 1c), a Fraunhofer diffraction setup is implemented on the other side of the ESI source and the same excitation laser is used. A system of two cylindrical lenses is used to direct the diffracted light on the Charge Coupled Device (CCD) camera guppy F-080B/C FireWire (Allied Vision Technologies, Stadtroda, Germany). The first lens (f = 100 mm) allows the collection of the scattered light for a solid angle ranging from $\boldsymbol{\theta_{min}}$ = 6.7° to $\boldsymbol{\theta_{max}}$ = 17.7° with respect to the laser beam axis, whereas the second one (f = 150 mm) is used to focus the light on the CCD camera. The

Table 2. Change of MeCN content and $pH_{abs}^{H_2O}$ in the ESI plume ($y = 3$ mm), $x_{max} = 15$ mm from the needle tip, except for 50% MeCN initial content, Where $x_{max} = 13$ mm

Initial MeCN content	80%	80%	80%	80%	50%	50%
Initial ${}_w^wpH$	4.00	4.00	5.03	5.03	5.03	5.03
Initial $pH_{abs}^{H_2O}$	7.64	7.64	8.43	8.43	7.05	7.05
ESI mode	ESI+	ESI−	ESI+	ESI−	ESI+	ESI−
ΔMeCN content % (percentage point)	5.6%	5.7%	5.3%	7.4%	7.0%	7.5%
$pH_{abs}^{H_2O}$ (${}_w^wpH$) at $x = 0$ mm	7.47 (3.78)	7.81 (4.27)	8.20 (4.80)	8.49 (5.14)	6.83 (4.82)	7.19 (5.16)
$pH_{abs}^{H_2O}$ (${}_w^wpH$) at x_{max}	6.66 (3.21)	7.19 (3.91)	7.52 (4.28)	7.82 (4.73)	6.28 (4.54)	6.62 (4.88)
Δ $pH_{abs}^{H_2O}$ (Δ${}_w^wpH$) in ESI plume	0.81 (0.57)	0.62 (0.36)	0.68 (0.52)	0.67 (0.41)	0.55 (0.28)	0.57 (0.28)

exposure time is set to 80 ms (with a time base of 20 µs) and 20 images are recorded for each point.

After plotting the signal intensity as a function of the scattering angle, using a homemade software, comparison with the Mie theory [33] allowed us to obtain the droplet size with accuracy better than 2.5% due to the high sensitivity of the interference pattern to the size for µm-sized droplets.

The obtained fluorescence spectra is an average of droplets present in the size of the laser beam (~1 mm). So the pH and mobile phase composition measured correspond to an area of ~0.78 mm^2 in the ESI plume and not for a unique droplet.

The temperature of the droplets was not profiled in this study. However previous studies performed with methanol droplets have shown either a slight increase of temperature [19] or some decrease [34] along the plume. The temperature of the plume in the referred studies was found to be between 295 and 307 K.

Compounds

The fluorescent pH indicator 5(6)-carboxy-2',7'-dichlorofluoresceine (Sigma, ≥95%) and solvatochromic Nile Red (Invitrogen, Cergy, Pontoise, France) were used as fluorescent probes. Acetonitrile (J.T.Baker, Deventer, Netherlands, HPLC grade), MilliQ water (Millipore Advantage A10 MILLIPORE GmbH, Molsheim, France), formic acid (Fluka, 98%, Buchs, Switzerland), ammonium hydroxide (Lach:Ner, 25%, Czech Republic), dimethyl sulphoxide (Sigma,

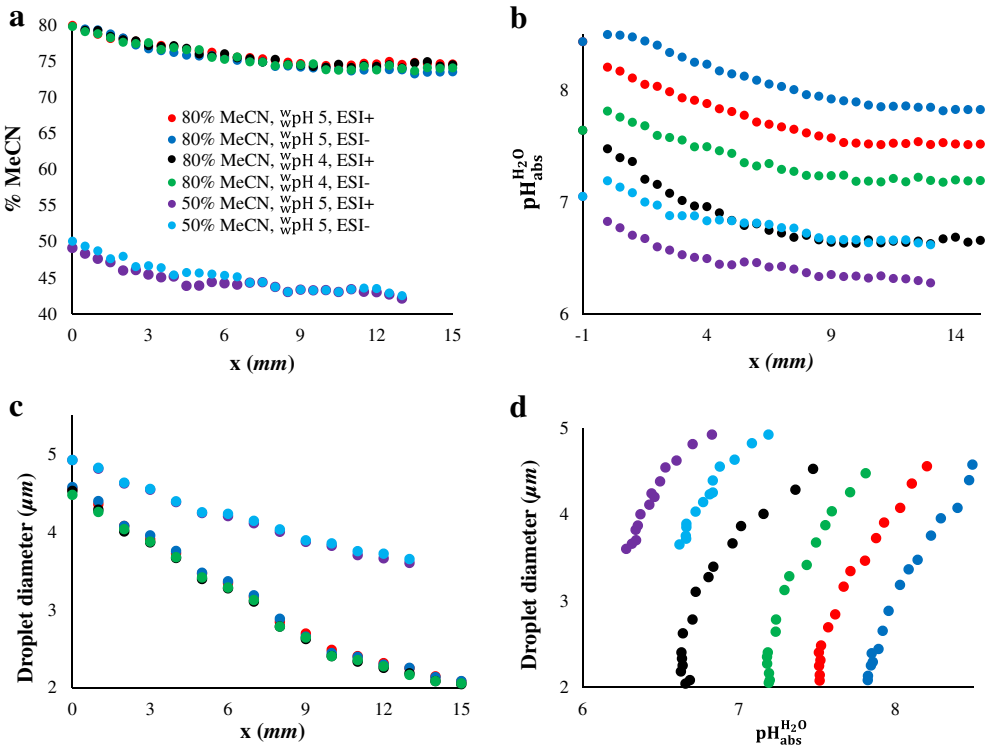

Figure 1. Change in (a) MeCN content in the middle of the ESI plume ($y = 3$ mm), (b) $pH_{abs}^{H_2O}$ in the middle of the plume. pH in $x = -1$ mm is the $pH_{abs}^{H_2O}$ of the initial mobile phase, (c) average droplet diameter in the spray plume versus the axial distance x from the emitter tip (average error is ±0.6 µm), (d) average droplet diameter versus the $pH_{abs}^{H_2O}$ in ESI plume. The legend is the same for a, b, c, and d

Steinheim, Germany), buffer pH 7.00 (Fluka, Buchs, Switzerland) were used. Water phase pH values ($^{w}_{w}$pH) were measured with Hanna Instruments pH211 Microprocessor pH Meter equipped with a 4 mm-diameter microelectrode (Pt//3.5 mol/L KCl+AgCl).

First of all, the chromism of Nile Red (20 μM) was calibrated in MeCN/water binary solvent mixtures. Variation in the MeCN/water ratio induces a shift of the maximum emission wavelength. The solvent composition of an unknown solution can be determined based on the λ_{max} using the calibration curve.

For pH measurements, stock solutions containing 0.1 mM of 5(6)-carboxy-2',7'-dichlorofluoresceine were made in dimethyl sulphoxide. From the initial solution, 10 μM binary acetonitrile/water solutions were prepared, where the $^{w}_{w}$pH varied: 3.50, 4.00, 4.50, 5.03, 5.52, 6.04, and 6.51. Water phase solutions were prepared by first making 0.1% formic acid solution and then adjusting pH by adding the 25% ammonium hydroxide solution to the desired $^{w}_{w}$pH. The obtained water phase solutions were then mixed in different ratios with acetonitrile so that acetonitrile content in the calibration solutions was 80%, 75%, 70%, 65%, 60%, 55%, 50%, 45%, 40%. In order to establish calibration curves, fluorescence spectra of all the obtained 63 mixtures were measured, in solution and logarithm of the ratios of fluorescence emission intensities was calculated.

Results

The results of MeCN content and $pH^{H_2O}_{abs}$ change in the ESI plume for all studied mobile phases are presented in Table 2. In all cases, the MeCN content decrease across the plume is 5.3 to 7.5% (percentage point), as acetonitrile is more readily vaporized during the evaporation process of the droplets. These changes in MeCN content in the ESI plume have been taken into account for the determination of the pH. This means for every point in the pH calibration curve the corresponding MeCN content percentage was used. For all mobile phases the ESI+ mode has somewhat smaller change in MeCN content, however the difference is statistically insignificant.

The $pH^{H_2O}_{abs}$ at the ESI needle tip (x = 0 mm) is different (confirmed by t-test) from the $pH^{H_2O}_{abs}$ of the initial bulk solution (Table 2). The $pH^{H_2O}_{abs}$ difference of 0.06 to 0.23 pH units is observed between the bulk mobile phase and mobile phase in the needle tip. The $pH^{H_2O}_{abs}$ change along the plume is visualized in Figure 1b. It can be observed that the $pH^{H_2O}_{abs}$ of the solution decreases steadily along the ESI plume (i.e. becomes more acidic). In the case of a 50% MeCN content in the initial solution, the change in the pH is lower than for 80% initial MeCN content. The droplets for 50/50 acetonitrile/$^{w}_{w}$pH 5.00 water phase are more acidic according to $pH^{H_2O}_{abs}$ than for 80/20 acetonitrile/$^{w}_{w}$pH4.00. This demonstrates that $^{w}_{w}$pH alone is not suitable for describing the acidity of mobile phase.

The largest difference of the $pH^{H_2O}_{abs}$ for ESI+ and ESI- down the plume evolution was observed for mobile phase containing 80/20 MeCN/$^{w}_{w}$pH 4.00 and the change was up to 0.81 pH units.

The droplet size was determined by Mie scattering measurements. The comparison of the projection of the signal intensity as a function of the scattering angle with the Mie theory allows determining the average droplet diameter at each point in the ESI plume, for the previously determined solvent compositions. The droplets shrink as they move downstream because of the evaporation process. Note that the reported droplet size is an average of the size of droplets within a pixel, which is an area of 500 μm × 500 μm. Moreover, the droplets constituting the ESI plume are polydisperse. The droplet size distribution for each pixel is found to be Gaussian with a standard deviation σ ranging from 1 to 2.5%. The droplet diameter is decreasing along the plume from 4.5 μm to 2 μm for the MeCN/water 80/20 solvent mixture. For the 50/50 mixture, the initial droplet diameter is higher (4.9 μm) and the solvent evaporation is less efficient, leading to droplet diameter of 3.6 μm at x = 13 mm from the emitter tip. However, droplet size measurements demonstrate that droplet diameter change is independent of the ESI mode.

Discussion

In this paper, we present the study of the ESI plume with most acidic mobile phase profiled so far. In ESI+, acidic mobile phases are much more often used than neutral or basic mobile phases and are therefore of great interest. The main difficulty was to find a dye with low enough pK_a value, with acceptable solubility in the mobile phase and significant change of spectral features with pH. The lowest pH that could be profiled with the used dye was $^{w}_{w}$pH of 3.00.

Secondly, in this paper for the first time we simultaneously measure plume parameters for ESI+ [16, 27, 34] and ESI– [14] with exactly the same ESI source setup and with mixtures containing also organic solvent. Previous analogous measurements were carried out using different conditions, instrumentation, measurement method, etc., thus not allowing direct comparison of the processes in ESI+ and ESI– for common mobile phases.

Thirdly, it is the first time plume profiling is connected with unified pH ($pH^{H_2O}_{abs}$) measurements. Expressing mobile phase acidity as $pH^{H_2O}_{abs}$ allows comparing acidities of plumes with different organic solvents and different organic solvent content. This makes the results of this work also comparable with future research, independent of the mobile phase being used.

The droplets profiled in this study are the large parent droplets (in a micrometer scale) observed in the ESI plume. They are in different stages of development: (1) approaching Rayleigh limit, (2) close to the Rayleigh limit, and (3) already undergone Coulomb explosion and emitted significant amount of excess charge via formation of smaller offspring droplets.

Therefore not all of the droplets are at the same stage and profiling gives us the average of these droplets.

The mobile phase becomes more acidic (compared with the initial acidity) at the needle tip (x = 0 mm) in the ESI+ mode, whereas in ESI– it becomes more basic. The acidities at this point are not yet influenced by the selective evaporation that occurs in the plume, as the measurements are made directly in the needle tip. This is also observable on Figure 1a, which shows the acetonitrile content along the plume starting from the needle tip. The change in $pH_{abs}^{H_2O}$ is caused by the electrochemical reactions taking place in the very end on the needle capillary. In ESI+ mode the electrochemical reaction creates an additional amount of protons from water or additives, whereas in ESI– hydroxyl ions are generated or protons are neutralized [10–12, 35, 36].

The $pH_{abs}^{H_2O}$ change occurring between bulk phase and droplets in the needle tip is significant. However, the absolute value of $pH_{abs}^{H_2O}$ change is very similar for ESI+ (up to 0.23 units) and ESI– (up to 0.17 units). Therefore, the absolute differences in the changes of $pH_{abs}^{H_2O}$ occurring in the needle tip for ESI+ and ESI– are insignificantly different statistically. Based on this, it is impossible to decide the efficiency of electrochemical reaction between ESI modes and mobile phases. Van Berkel et al. [35] have previously found and calculated that the change could be in the order of 2 or more pH units. This may result from the fact that in their study pure water without buffering agent was used.

It is worth mentioning though that the $pH_{abs}^{H_2O}$ differences are much smaller than have been predicted by theoretical calculations [25]. A probable reason is that calculations can only be made based on the assumption of reached equilibria. However, it is important to note that it is not known whether the droplets formed in ESI are actually in their equilibrium. In previous studies, it has been shown that some compounds may retain their liquid-phase structures (charge location) due to kinetical trapping [37] – meaning that the drying of the droplets in ESI is too fast for the droplets to reach the actual equilibrium. Therefore, it is also likely that at least some of the droplets profiled in our work have not reached the chemical equilibria (including acid–base equilibrium).

For all studied mobile phases and in both modes it was observed that the solutions become more acidic along the plume. This is caused by more ready vaporization of acetonitrile and the resulting decrease of the content of MeCN in the droplets along the plume, causing an increase of water content. Three different factors operate here: (1) increase of formic acid (the aqueous phase consists of 0.1% formic acid solution titrated with 25% ammonia solution to the desired pH) acidity (decrease of pK_a); (2) increase of formic acid concentration in solution, and (3) further increase of the share of the (more basic) water in the solvation sphere. While the last factor causes decrease of the solvated proton activity, the first two outweigh it, causing altogether the increase of acidity. The influence of solvent composition change on basicity of ammonia is less important because (1) basicity of bases is less influenced by adding organic solvent [29], and (2) the used pH range is far from the pK_a of NH_4^+. The pH change in the plume is in general similar to that expected and also previously demonstrated [12]. Therefore, indicating that tendencies found previously for neutral and basic mobile phases are also valid for acidic mobile phases.

The decrease of $pH_{abs}^{H_2O}$ along the plume is very similar in ESI+ and ESI– resulting in almost parallel evolution of lines within one mobile phase in Figure 1b. Therefore, the $pH_{abs}^{H_2O}$ difference for ESI+ and ESI– generated by the electrochemical reaction in the needle tip remains essentially the same throughout the plume in spite of acetonitrile evaporation. Only in the case of aqueous phase with ${}^{w}_{w}pH$ of 4.00 is the change in acidity greater in ESI+ than in ESI–, causing the $pH_{abs}^{H_2O}$ difference of 0.53 units at the maximum profiling length between different modes. If electrochemical reactions would be of the same efficiency for all mobile phases and the organic solvent evaporation rates would be indistinguishable, as observed form Figure 1a, we would expect that more acidic mobile phase obeys less pH change than the less acidic (also keeping in mind that the buffering capacity for this studied mobile phase is much higher).

Also, it was observed that $pH_{abs}^{H_2O}$ change is larger for mobile phase containing 80% of acetonitrile than for mobile phase containing 50% of acetonitrile. The probable reasons could be: (1) the profiled length is longer (15 mm versus 13 mm in the case of 50% MeCN), and (2) the change in the droplet size is larger (Figure 1c and d). The first possibility may be ruled out, as the plateau of the pH change has already been achieved at x = 13 mm. The droplet size change, however, is in almost linear relation with $pH_{abs}^{H_2O}$ (see Figure 1d). It is observed that the droplet size changes more for mobile phase with 80% of MeCN than with 50% of MeCN. MeCN evaporates more readily from solution with higher MeCN content [14]: both 50/50 and 80/20 mobile phases lose about 5% of acetonitrile; therefore the total acetonitrile loss (and thereby the increase in water content leading to increased dissociation of formic acid) for the latter is higher. Solvent fractionation is less efficient when the initial water content is higher.

The method used allows us to profile the droplets down to 0.5 μm in diameter, therefore indicating two mechanisms influencing the plume evolution. First, the drying of the droplets due to heated drying gas: in this process the more volatile mobile phase component evaporates faster, but the changes are expected to be similar for the two ESI modes. Secondly, the fission of the charged nanodroplets from the parent droplets: this mechanism can have an effect on the composition of the remaining part of the parent droplet and is expected to influence ESI+ and ESI– mode differently. In ESI+ and ESI– ions of different type are removed from the parent droplets during ejection of nanodroplets, therefore facilitating $pH_{abs}^{H_2O}$ change in different directions. Each fission of one nanodroplets removes 10% to 40% of the excess charge (depending on the solvent) from the parent droplet [38–41]. The general amount of excess charge can be estimated on the basis of pH change from bulk mobile phase to mobile phase in the needle tip. Therefore, if the fission of nanodroplets would be a dominant process changing the composition of the parent droplets, we

would expect: (1) a significantly different $pH_{abs}^{H_2O}$ profiles for ESI+ and ESI– along the plume, and (2) more significant changes in the droplets $pH_{abs}^{H_2O}$ along the plume.

These findings are important from two aspects. First, for modeling ESI process, these findings demonstrate that desolvation due to drying dominates over the fission of nanodroplets in case of pneumatically assisted ESI sources. This means that similar models for ESI+ and ESI– mode can theoretically be constructed, and this could also serve as a validation criterion for such models. Secondly, for practitioners these findings show that qualitative findings related to the ESI process obtained on the ESI+ mode can almost directly be applied also in the ESI– mode. However, the importance of desolvation gas is enormous and therefore quantitative findings are transferable only within one set of gas parameters between ESI+ and ESI–.

Conclusions

The mobile phase with the most acidic pH was profiled, and it was demonstrated that the changes are in accordance with similar measurements carried out for neutral and basic mobile phases. Changes in organic content percentage, pH, and droplet size are very similar for both ESI+ and ESI–, indicating that in these methods, the two modes are similar. In all cases, mobile phases became more acidic along the plume, but less than predicted by calculations. These experiments demonstrate that the dominant mechanism influencing plume evolution is desolvation due to drying. The results aid in understanding the conditions of where the ionization occurs better and enables directly comparing the two polarities used for ESI ionization efficiency measurements. This is very promising; our group is currently working on establishing a solid quantitative link between the ionization efficiencies in the two ionization modes, which would enable deciding whether ESI+ or ESI– is more promising for a given analyte.

Acknowledgements

This work was supported by Personal Research Funding Project 34 from the Estonian Research Council, and by national scholarship program Kristjan Jaak, which is funded and managed by the Archimedes Foundation in collaboration with the Ministry of Education and Research. The research leading to these results has received funding from Agilent Technologies with an award through Agilent's Application and Core Technology University Research Program (grant ID 2243). The work of A.H. and I.L. was supported by the Institutional funding project IUT20-14 from the Estonian Ministry of Education and Research.

References

1. Cech, N.B., Enke, C.G.: Practical implications of some recent studies in electrospray ionization fundamentals. Mass Spectrom. Rev. **20**, 362–387 (2001)
2. Cole, R.B.: Electrospray and MALDI mass spectrometry: fundamentals, instrumentation, practicalities, and biological applications. Wiley, Hoboken (2010)
3. Kruve, A.: Influence of mobile phase, source parameters, and source type on electrospray ionization efficiency in negative ion mode: influence of mobile phase in ESI/MS. J. Mass Spectrom. **51**, 596–601 (2016)
4. Zhou, S., Hamburger, M.: Effects of solvent composition of molecular ion response in electrospray mass spectrometry: investigation of the ionization process. Rapid Commun. Mass Spectrom. **9**, 1516–1521 (1995)
5. Liigand, J., Laaniste, A., Kruve, A.: pH effects on electrospray ionization efficiency. J. Am. Soc. Mass Spectrom. **28**, 461–469 (2017)
6. Zhou, S., Cook, K.D.: Protonation in electrospray mass spectrometry: wrong-way-round or right-way-round? J. Am. Soc. Mass Spectrom. **11**, 961–966 (2000)
7. Oss, M., Kruve, A., Herodes, K., Leito, I.: Electrospray ionization efficiency scale of organic compounds. Anal. Chem. **82**, 2865–2872 (2010)
8. Liigand, J., Kruve, A., Leito, I., Girod, M., Antoine, R.: Effect of mobile phase on electrospray ionization efficiency. J. Am. Soc. Mass Spectrom. **25**, 1853–1861 (2014)
9. Kruve, A., Kaupmees, K., Liigand, J., Leito, I.: Negative electrospray ionization via deprotonation: predicting the ionization efficiency. Anal. Chem. **86**, 4822–4830 (2014)
10. Zhou, S., Edwards, A.G., Cook, K.D., Van Berkel, G.J.: Investigation of the electrospray plume by laser-induced fluorescence spectroscopy. Anal. Chem. **71**, 769–776 (1999)
11. Zhou, S., Prebyl, B.S., Cook, K.D.: Profiling pH changes in the electrospray plume. Anal. Chem. **74**, 4885–4888 (2002)
12. Girod, M., Dagany, X., Antoine, R., Dugourd, P.: Relation between charge state distributions of peptide anions and pH changes in the electrospray plume. a mass spectrometry and optical spectroscopy investigation. Int. J. Mass Spectrom. **308**, 41–48 (2011)
13. Girod, M., Antoine, R., Dugourd, P., Love, C., Mordehai, A., Stafford, G.: Basic vapor exposure for tuning the charge state distribution of proteins in negative electrospray ionization: elucidation of mechanisms by fluorescence spectroscopy. J. Am. Soc. Mass Spectrom. **23**, 1221–1231 (2012)
14. Girod, M., Dagany, X., Boutou, V., Broyer, M., Antoine, R., Dugourd, P., Mordehai, A., Love, C., Werlich, M., Fjeldsted, J., Stafford, G.: Profiling an electrospray plume by laser-induced fluorescence and Fraunhofer diffraction combined to mass spectrometry: influence of size and composition of droplets on charge-state distributions of electrosprayed proteins. Phys. Chem. Chem. Phys. **14**, 9389–9396 (2012)
15. Zhou, S., Cook, K.D.: Probing solvent fractionation in electrospray droplets with laser-induced fluorescence of a solvatochromic dye. Anal. Chem. **72**, 963–969 (2000)
16. Wang, R., Zenobi, R.: Evolution of the solvent polarity in an electrospray plume. J. Am. Soc. Mass Spectrom. **21**, 378–385 (2010)
17. Hopkins, R.J., Reid, J.P.: Evaporation of ethanol/water droplets: examining the temporal evolution of droplet size, composition, and temperature. J. Phys. Chem. A **109**, 7923–7931 (2005)
18. Wortmann, A., Kistler-Momotova, A., Zenobi, R., Heine, M.C., Wilhelm, O., Pratsinis, S.E.: Shrinking droplets in electrospray ionization and their influence on chemical equilibria. J. Am. Soc. Mass Spectrom. **18**, 385–393 (2007)
19. Soleilhac, A., Dagany, X., Dugourd, P., Girod, M., Antoine, R.: Correlating droplet size with temperature changes in electrospray source by optical methods. Anal. Chem. **87**, 8210–8217 (2015)
20. Oh, M.I., Consta, S.: Stability of a transient protein complex in a charged aqueous droplet with variable pH. J. Phys. Chem. Lett. **8**, 80–85 (2017)
21. Sharawy, M., Consta, S.: How do noncovalent complexes dissociate in droplets? A case study of the desolvation of dsDNA from a charged aqueous nanodrop. Phys. Chem. Chem. Phys. **17**, 25550–25562 (2015)
22. Ahadi, E., Konermann, L.: Molecular dynamics simulations of electrosprayed water nanodroplets: internal potential gradients, location of excess charge centers, and "hopping" protons. J. Phys. Chem. B **113**, 7071–7080 (2009)
23. Sharawy, M., Consta, S.: Characterization of "star" droplet morphologies induced by charged macromolecules. J. Phys. Chem. A **120**, 8871–8880 (2016)
24. Consta, S., Oh, M.I., Malevanets, A.: New mechanisms of macro-ion-induced disintegration of charged droplets. Chem. Phys. Lett. **663**, 1–12 (2016)
25. Malevanets, A., Consta, S.: Variation of droplet acidity during evaporation. J. Chem. Phys. **138**, 184312 (2013)

26. Chillier, X.F.D., Monnier, A., Bill, H., Gulacar, F.O., Buchs, A., McLuckey, S.A., Van Berkel, G.J.: A mass spectrometry and optical spectroscopy investigation of gas-phase ion formation in electrospray. Rapid Commun. Mass Spectrom **10**, 299–304 doi:10.1002/(SICI)1097-0231(199602)10:3<299::AID-RCM502>3.0.CO;2-U
27. Davis, D., Portelius, E., Zhu, Y., Feigerle, C., Cook, K.D.: Profiling an electrospray plume using surface-enhanced raman spectroscopy. Anal. Chem. **77**, 8151–8154 (2005)
28. Himmel, D., Goll, S.K., Leito, I., Krossing, I.: Anchor points for the unified Brønsted acidity scale: the rCCC model for the calculation of standard Gibbs energies of proton solvation in eleven representative liquid media. Chem. Eur. J. **17**, 5808–5826 (2011)
29. Suu, A., Jalukse, L., Liigand, J., Kruve, A., Himmel, D., Krossing, I., Rosés, M., Leito, I.: Unified pH values of liquid chromatography mobile phases. Anal. Chem. **87**, 2623–2630 (2015)
30. Buck, R., Rondinini, S., Covington, A., Baucke, F., Brett, C., Camoes, M., Milton, M., Mussini, T., Naumann, R., Pratt, K., Spitzer, P., Wilson, G.: Measurement of pH. definition, standards, and procedures. Pure Appl. Chem. **74**, 2169–2200 (2002)
31. Himmel, D., Goll, S.K., Leito, I., Krossing, I.: A unified pH scale for all phases. Angew. Chem. Int. Ed. **49**, 6885–6888 (2010)
32. Mussini, T., Covington, A.K., Longhi, P., Rondinini, S.: Criteria for standardization of pH measurements in organic solvents and water + organic solvent mixtures of moderate to high permittivities. Pure Appl. Chem. **57**, 865–876 (1985)
33. Bohren, C.F., Huffman, D.R.: Absorption and scattering of light by small particles. Wiley-VCH Verlag GmbH & Co. KGaA, Weinheim (1998)
34. Gibson, S.C., Feigerle, C.S., Cook, K.D.: Fluorometric measurement and modeling of droplet temperature changes in an electrospray plume. Anal. Chem. **86**, 464–472 (2014)
35. Van Berkel, G.J., Zhou, F., Aronson, J.T.: Changes in bulk solution pH caused by the inherent controlled-current electrolytic process of an electrospray ion source. Int. J. Mass Spectrom. Ion Process. **162**, 55–67 (1997)
36. de la Mora, J.F., Van Berkel, G.J., Enke, C.G., Cole, R.B., Martinez-Sanchez, M., Fenn, J.B.: Electrochemical processes in electrospray ionization mass spectrometry. J. Mass Spectrom. **35**, 939–952 (2000)
37. Seo, J., Warnke, S., Gewinner, S., Schöllkopf, W., Bowers, M.T., Pagel, K., von Helden, G.: The impact of environment and resonance effects on the site of protonation of aminobenzoic acid derivatives. Phys. Chem. Chem. Phys. **18**, 25474–25482 (2016)
38. Kebarle, P., Peschke, M.: On the mechanisms by which the charged droplets produced by electrospray lead to gas phase ions. Anal. Chim. Acta **406**, 11–35 (2000)
39. Peschke, M., Verkerk, U.H., Kebarle, P.: Features of the ESI mechanism that affect the observation of multiply charged noncovalent protein complexes and the determination of the association constant by the titration method. J. Am. Soc. Mass Spectrom. **15**, 1424–1434 (2004)
40. Kebarle, P., Verkerk, U.H.: Electrospray: from ions in solution to ions in the gas phase, what we know now. Mass Spectrom. Rev. **28**, 898–917 (2009)
41. Enke, C.G.: A predictive model for matrix and analyte effects in electrospray ionization of singly-charged ionic analytes. Anal. Chem. **69**, 4885–4893 (1997)